IN-05

3938602

TECHNICAL TRANSLATION
F-55

RESPONSE OF A HELICOPTER ROTOR TO AN INCREASE IN COLLECTIVE

PITCH FOR THE CASE OF VERTICAL FLIGHT

By Jean Rebont, Jacques Valensi, and Jean Soulez-Larivière

NATIONAL AERONAUTICS AND SPACE ADMINISTRATION

WASHINGTON   January 1961

[

RESPONSE OF A HELICOPTER ROTOR TO AN INCREASE IN COLLECTIVE

PITCH FOR THE CASE OF VERTICAL FLIGHT*

By Jean Rebont, Jacques Valensi, and Jean Soulez-Larivière

1. INTRODUCTION

The response to a change in collective pitch in descending flight
may be debased for certain flight conditions, the form being entirely
different according to whether the rapidity of the control application
is more or less great. The unsteady aerodynamic effect, which deter-
mines the form of the overall response, may be conveniently represented
by considering an apparent mass caused by temporary variations of the
induced velocity following a pitch change.

The present report gives an account of a theoretical and experi-
mental investigation of this subject at the Institute of Fluid Mechanics
of Marseilles, at the request of, and with the material support of, the
Rotating Wing Section of the Technical Service for Aeronautics. We
acknowledge, with gratitude, the kindness of the Director of Technical
Service for Aeronautics in authorizing the present publication, which
collects and completes information previously given in two Notes in
Compte Rendus of the Academy of Sciences[1].

The developed calculation should find application to the predic-
tion of the behavior of helicopters in landing. An analogous study,
conducted earlier in the United States[2], applies directly to the case

---

*Translation of "Réponse d'un rotor d'hélicoptère a une augmenta-
tion du pas général dans le cas du vol vertical." Technique et Science
Aéronautiques, no. 3, May-June 1959, pp. 177-183.

[1]Rebont, Jean, Valensi, Jacques, and Soulez-Larivière, Jean:
Réponse de la portance d'un rotor à une augmentation de pas général
dans le cas du vol de descente, le régime du rotor étant voisin
de l'autorotation. Compte Rendus, T. 247, no. 9, 1958, pp. 738-741,
and T. 247, no. 10, 1958, pp. 778-780, (available in English translation
as NASA TT F-17, 1960 and NASA TT F-18, 1960).

[2]Carpenter, Paul J., and Fridovich, Bernard: Effect of a Rapid
Blade-Pitch Increase on the Thrust and Induced Velocity Response of a
Full-Scale Helicopter Rotor. NACA TN 3044, 1953.

of vertical take-off for an overloaded helicopter. Despite a great
search of the literature, no similar study concerning landing was found
to exist.

2. NOTATION AND SYMBOLS

OX,OY,OZ   reference axes

OZ   perpendicular to the rotor disk

OX   in the direction of the translation velocity

F_n projection of the force in the direction OZ

U   tip speed

$\bar{F}_n$ $\dfrac{F_n}{\frac{1}{2}\rho SU^2}$

λ_i equivalent reduced induced velocity $\dfrac{V_i}{U}$

V   velocity

V_x, V_z projections of velocity at point O

$\lambda = \dfrac{V_z}{U}$ axial-flow ratio

$\mu = \dfrac{V_x}{U}$ advance ratio

θ section pitch at 0.7 radius

R   rotor radius

S   disk area of rotor

b_2 number of blades

l blade chord

$\sigma = \dfrac{b_2 l_{0.7}}{\pi R}$ rotor solidity which relates the blade area to the surface area of the disk

$\bar{G}_0, \bar{G}_1, \bar{G}_2$ blade form parameters

$$\bar{G}_0 = \frac{\int_0^R l\ dr}{l_{0.7} R}$$

$$\bar{G}_1 = \frac{\int_0^R lr\ dr}{l_{0.7} R^2}$$

$$\bar{G}_2 = \frac{\int_0^R lr^2 dr}{l_{0.7} R^3}$$

$$\left.\begin{array}{l} \bar{G}_0 = 1 \\[6pt] \bar{G}_1 = \dfrac{1}{2} \\[6pt] \bar{G}_2 = \dfrac{1}{3} \end{array}\right\} \text{ rectangular blades}$$

$\bar{L}_0, \bar{L}_1, \bar{L}_2$ blade twist parameters

$$\bar{L}_0 = \frac{\int_0^R l\ \Delta\theta\ dr}{l_{0.7} R}$$

$$\bar{L}_1 = \frac{\int_0^R lr\ \Delta\theta\ dr}{l_{0.7} R^2}$$

$$\bar{L}_2 = \frac{\int_0^R lr^2 \Delta\theta\ dr}{l_{0.7} R^3}$$

4

$\dfrac{dC_z}{di}$ section lift-curve (in radians)

m   apparent mass

M   mass of helicopter

$$b = \dfrac{8}{3\,\dfrac{dC_z}{di}\,\sigma\overline{G}_2}$$

$$\tau = \dfrac{mb}{2\rho SU}$$

$$\tau_2 = \dfrac{Mb}{2\rho SU}$$

$$\tau^* = \dfrac{\tau}{b_1}$$

$$b_1 = bK_1 + \dfrac{2\overline{G}_1}{3\overline{G}_2}$$

$$E = \overline{G}_2 - \dfrac{2\overline{G}_1}{3b_1}$$

$$F = \dfrac{2\overline{G}_1\tau^*}{3b_1(\tau^* - \alpha)}$$

$$H = -\overline{G}_2 + \dfrac{2\alpha\overline{G}_1}{3b_1(\tau^* - \alpha)}$$

$$H_s = -\left(\overline{G}_2 - \dfrac{2\overline{G}_1}{3b_1}\right)$$

$$F^* = \dfrac{\overline{F}_{n_t \to \infty} - \overline{F}_{n_{t=0}}}{\dfrac{dC_z}{di}\,\sigma A}$$

$$\Delta^* = \frac{3\left(\overline{G}_2 - F^*\right)^2}{2\overline{G}_1 F^*}$$

A, α amplitude and time constant of pitch change

3. EQUATIONS FOR LIFT IN THE UNSTEADY REGIME

Consider the approach to the case of steady rising flight. A classical calculation leads to an approximate expression for $\overline{F}_n$ as a function of θ, λ, and λ_i, which combines with the equation deduced by blade-element theory, when blade flapping has no effect, to give

$$\overline{F}_n = \frac{dC_z}{di} \sigma \left[\theta \overline{G}_2 - \overline{G}_1\left(\lambda + \lambda_i\right) + \overline{L}_2\right] \tag{1}$$

which is deduced[3] from the elementary theory of Froude; that is

$$\overline{F}_n = 4\lambda_i\left(\lambda_i + \lambda\right) \tag{2}$$

For the case of descending flight near the autorotative state, one can follow an analogous process for the calculation of the response in lift in the transient state to a not too violent increase in collective pitch. Under this restriction, one may consider equation (1) to remain valid as regards the aerodynamic forces on the element, thus determining a function of the instantaneous motion by the same laws as in the steady state. Nevertheless, it is necessary to utilize a differential equation in place of equation (2) in order to simultaneously account for the initial state (descending flight), and for the instantaneous change of the induced velocity field resulting from the change in pitch.

In the instant preceding application of the control demand, the air outlines the rotor disk, which itself behaves approximately as a solid disk. Immediately after the application of the control demand, a certain mass of air, which outlines and is situated above the disk, as shown in the collection of photographs of the present report, is brought back through the disk in an eddying motion, and it then grows

[3]Legrand, F.: Gyroplanes. Course at the Ecole Nationale Supérieure d'Aéronautique, 1958.

again below the disk. Thus a new induced velocity field tends to be established across the width of the disk.

At the end of a certain time (theoretically infinite, but, in practice, limited), the field attains its final configuration. It corresponds to the final value of the lift. This value may be calculated by means of equation (1) if θ is given in its final value and if the preceding equation of Froude, valid only for climbing flight, is replaced by an equation for the mass flow in the steady state. It is not possible to establish this equation by simple reasoning except for climbing flight. It is necessary to have recourse to experience in order to find an empirical relation between F_n, λ, μ, and λ_i. Indeed, it will suffice to use the well-known, experimentally established charts of Oliver[4] who deduced λ_i, from the form $\frac{\overline{F_n}}{4} = f(\lambda_i)$, as a system of curves of constant λ for known values of μ. An example of these charts, corresponding to $\mu = 0$, is given in figure 1. The second equation then may be written formally as

$$\overline{F}_n = 4f(\lambda_i) \tag{3}$$

The solution of this system of two equations may be accomplished numerically, provided that an analytical representation of the useful portion of the curves is taken as a second degree equation, such as: $\overline{F}_n = 4K_1\lambda_i^2 + 4K_2\lambda\lambda_i + K_3$, with a suitable choice of the constants K_1, K_2, and K_3

In order to calculate $\overline{F}_n$ in the transient state, note that an inertia force is manifested by the rotor, resulting from the acceleration imposed on the mass of fluid affected by the vortex ring motion. This inertia force may be assimilated by a certain fluid mass, corresponding to the so-called "apparent mass," which is accelerated uniformly to $\lambda_i U$.

Then, by use of a new set of equations, constituted by the preceding equation (1) and by a new equation for the flow quantity, which is

$$\overline{F}_n = 4f(\lambda_i) + \frac{m\dot{\lambda}_i}{\frac{1}{2}\rho SU} \tag{4}$$

[4]Oliver, A.: The Low Speed Performance of a Helicopter. Rep. No. AAEE RES/264/1952.

the following is obtained:

$$\bar{F}_n = 4K_1\lambda_i^2 + 4K_2\lambda\lambda_i + 4K_3 + \frac{m\dot{\lambda}_i}{\frac{1}{2}\rho SU} \qquad (4)'$$

By elimination of $\bar{F}_n$ between equations (1) and (4), one nonlinear differential equation of the first order in λ_i is obtained.

$$\tau\dot{\lambda}_i = -bf(\lambda_i) + \frac{2\bar{G}_1\lambda_i}{3\bar{G}_2} + \frac{2\theta}{3} - \frac{2\bar{L}_2}{3\bar{G}_2} - \frac{2}{3}\frac{\bar{G}_1\lambda}{\bar{G}_2} \qquad (5)$$

This equation, upon the use of (4)' rather than (4), as well as the initial conditions: $\xi_{t=0} = \xi_0$, $\dot{\xi}_{t=0} = 0$, $\theta_{t=0} = \theta_0$, becomes

$$\tau\dot{\xi} = \frac{2}{3}(\theta - \theta_0) - bK_1\left(\xi^2 - \xi_0^2\right) \qquad (6)$$

where the new variable ξ is defined as

$$\xi = \lambda_i + \frac{3b\bar{G}_2K_1}{l\bar{G}_1} + \frac{l\lambda K_2}{2K_1} \qquad (7)$$

Equation (6) has the form of Riccati's equation.

4. INTEGRATION OF THE DIFFERENTIAL EQUATION: DISCUSSION

4.1. Large Increase in Collective Pitch

Equation (5), complete with its initial conditions, $\theta_{t=0} = \theta_0$; $(\lambda)_{t=0} = \lambda_0$; $(\lambda_i)_{t=0} = \lambda_{i_0}$; $(\dot{\lambda}_i)_{t=0} = 0$, equally as well as equation (6), may be handled by a numerical integration approach, the method of isoclines, once θ is substituted as a given function of time. In general, set

$$\theta = \theta_0 + A\left(1 - e^{-\frac{t}{\alpha}}\right) \qquad (8)$$

However, it is preferable to use equation (6) for discussing the form of the solutions. The calculations show that the appearance of F_n in the transient state depends essentially on α, or rather on $\frac{\alpha}{\tau}$,

8

that is to say, on the speed of the collective pitch change, the influence of which is most pronounced when ξ_C is very close to zero.

Of the numerous cases treated, three examples are given for a two-bladed rotor having no twist and having solidity $\sigma = 0.06$. The results, for the lift augmentation coefficient $\dfrac{\overline{F}_n - \overline{F}_{n_0}}{\overline{F}_{n_\infty} - \overline{F}_{n_0}}$ as a function of reduced time $\dfrac{t}{\tau}$ are given in figure 2.

The calculation parameters, that is, ξ_0 and $\dfrac{\alpha}{\tau}$, are indicated on the figure. A and λ were chosen as constants, and for the three examples, are equal to 0.14 and -0.05 radian, respectively.

The region of interest which is to be explored may be considered as characterized by $0 \leqq \xi_0 \leqq 0.03$, thus extending from the vortex ring to the windmill brake state and on one side of the regime of practical autorotation characterized by $\xi_0 \cong 0.03$. The case $\xi_0 = 0$ is presented as an extreme case and is not encountered in practice.

4.2. Small Increase in Collective Pitch (Less Than 5°)

The calculations may be greatly simplified for this case since, because the difference $\overline{F}_{n_\infty} - \overline{F}_{n_0}$ is small, a linear form may be used for $f(\lambda_i)$. Equation (5) may therefore be replaced by the following equation:

$$\overline{F}_n = 4K_1\lambda_i + 4K_3 + \frac{m\lambda}{\frac{1}{2}\rho SU} \tag{9}$$

This yields, as an expression for $\overline{F}_n$ in the transient state:

$$\overline{F}_n - \overline{F}_{n_{t=0}} = \frac{dC_z}{di}\,\sigma A\left[E + Fe^{-\frac{t}{\tau^*}} + He^{-\frac{t}{\alpha}}\right] \tag{10}$$

On the other hand, at any instant t, a fictitious lift $\overline{F}_{n_s}$ may be calculated by starting with equations (1) and (9) and suppressing the inertia terms in the second equation. $\overline{F}_{n_s}$ represents the lift which would be observed if equilibrium had been obtained at every instant in the transient state, or otherwise stated, the quasi-static lift for the instantaneous pitch θ.

The difference $\bar{F}_{n_{t,\theta}} - \bar{F}_{n_{s,\theta}}$ (fig. 3) represents the excess lift resulting from unsteady effects. It may be expressed as

$$\bar{F}_{n_{t,\theta}} - \bar{F}_{n_{s,\theta}} = \frac{dC_z}{di}\, \sigma A \left[Fe^{-\frac{\tau}{\tau^*}} + \left(H - H_s\right)e^{-\frac{t}{\alpha}} \right] \qquad (11)$$

The normalized impulse caused by unsteady effects may, by taking the time τ and the force $\bar{F}_{n_\infty} - \bar{F}_{n_0}$ as unity, be calculated as the increase in normalized lift between the initial and final states:

$$\Delta^* = \frac{\int_0^\infty \left(\bar{F}_n - \bar{F}_{n_s}\right) dt}{\left(\bar{F}_{n_\infty} - \bar{F}_{n_0}\right)\tau} \qquad (12)$$

which may be rewritten as

$$\Delta^* = \frac{3\left(\bar{G}_2 - F^*\right)^2}{2\bar{G}_1 F^*} \qquad (13)$$

where

$$F^* = \frac{\bar{F}_{n_\infty} - \bar{F}_{n_0}}{\dfrac{dC_z}{di}\, \sigma A}$$

The normalized impulse caused by the unsteady effects is merely a function of the increase in lift between initial and final states and of the form parameters $\bar{G}_1$ and $\bar{G}_2$.

Δ^* as a function of F^* is shown in figure 4 for a rotor with rectangular blades. It is evident that Δ^* is a function of the initial state; the normalized impulse due to unsteady effects is very much greater when the initial state is near autorotation than when near the vortex-ring state. This is an important result for control behavior in landing.

Finally, equation (10) allows the calculation of maximum effort as a function of F^* as determined by related values of τ/α. The calculated results are shown in figure 5 for the following values of $\frac{\tau}{\alpha}$: 4.09, 3, 1.8, 0.75, 0.459, and 0.30.

5. EXPERIMENTAL VERIFICATION

5.1. Description of Setup

A helicopter rotor was placed in the stream of the elliptical (3.30 x 2.20 m) wind tunnel of the Institute of Fluid Mechanics of the University of Aix-Marseille.

The setup (see figs. 6 and 7) consisted of the auxiliary rotor and transmission case of an S. E. 120. This was fixed to the end of a thin-walled steel tube placed horizontally in the working section with its axis coincident with and centered on the major axis of the section. The tube is connected to a fixed mount placed at the side of the air-stream by the medium of two bearings which allow orientation of the rotor disk. The drive shaft of the rotor passes through the tube; it has a tachometer and a rotating contact at its free end, thus permitting the operator to view every revolution of the rotor. The rotor is driven by a variable speed motor by means of 6 V-belts.

The pitch change is obtained automatically by means of an arrangement of cams which allow adjustment of the amplitude and speed of the pitch change (fig. 8).

Four wire strain gages are glued on the exterior surface of the tube in a standard arrangement. The blade flapping and collective pitch are measured by means of variable-reluctance angular trans-ducers. The signals are sent from the gage bridges and the angular pick-ups to an oscillograph where they are recorded along with a time base and a revolution counter.

The array of equipment is completed by a smoke-producing apparatus (ammonium chlohydrate) feeding 3 or 5 orifices through a distributor mounted above the rotor and by a drum-fed camera with a shutter con-trolled by the pitch change apparatus. The controlled light was very great and the film ran through the camera at the rate of one photograph per revolution throughout the entire pitch change.

5.2. Results

5.2.1. Collective pitch change of large amplitude.- Of the number of cases studied, three records are extracted and shown in figure 9. These correspond to the following conditions: rotor diameter, 2 meters; rotor angle of attack 90° (vertical flight); two rectangular blades without twist; solidity $\sigma = 0.085$; $\mu = 0$; $\xi_0 = 0.025$; amplitude of pitch change, $A = 0.158$ radian; $\frac{\alpha}{\tau}$ equal, respectively, to 0.33 for

figure 9(a), 2.1 for figure 9(b), 5.5 for figure 9(c); and $\tau = 0.038$. The tip speed was maintained at 180 meters per second and the wind-tunnel speed at 7.2 meters per second ($\lambda = -0.04$).

It may be seen that the lift response shows all of the characteristics predicted by theory. In particular, figure 9(b) shows the existence of a lift minimum after 9 rotor revolutions, whereas the following figure indicates that the limiting value was obtained after five revolutions. Significant blade flapping may be observed in figures 9(a) and 9(b), of amplitude $2°10'$ and $1°32'$, respectively.

The flapping is accompanied by intense noise, but it does not appear to have significant influence on the overall lift. It should be noted that the pitch increase was maintained for a time just sufficient to permit recording the phenomena, wholly in order to avoid giving too much importance to variations in wind-tunnel speed and rotor regime. The choice of time scale for the three figures was determined by the value of α.

5.2.2. Pitch change of small amplitude.- Records have been obtained for a two-bladed rotor of solidity $\sigma = 0.112$ and diameter of 1.5 meters. The amplitude of pitch change was held equal to 0.0785 radian, and Δ^* has been deduced as a function of F^*. The corresponding points have been placed on figure 4, which carries a legend giving the major variables characterizing the study. Note that calculation of Δ^* prior to the test implies an exact knowledge of the apparent mass.

If the apparent mass is taken, as in the preceding sections, as the apparent mass for a solid disk in nonuniform motion perpendicular to the disk, that is, $\overline{m}\frac{3}{4}\rho\pi R^3$ with $\overline{m} = 0.637$, the points do not fall properly on the curves. If a doubled value of $\overline{m}$ is adopted, all of the points, though corresponding to very different test conditions, fall much closer to the calculated curve.

It may be hoped that the value of $\overline{m}$ determined in this way represents the most probable value of this coefficient in the transient descending flight of a helicopter. Furthermore, the study has shown, by tests with a rotor, different characteristics, especially those concerning solidity, which permit verification of the validity of this determination.

Finally, by taking the preceding value, that is, 1.274 for $\overline{m}$, the experimental values of $\dfrac{\overline{F}_{n_{max}} - \overline{F}_{n_0}}{\overline{F}_{n_\infty} - \overline{F}_{n_0}}$ as a function of F^* for

12

various values of $\frac{x}{\alpha}$ are given in figure 5. The distribution of the experimental points presents new evidence of satisfactory agreement between theory and practice.

5.3. Photographs of the Flow

Figure 10 reproduces a sequence of views observed in the transient state under the conditions which are summarized in the legend. The initial conditions are close to the vortex-ring state and the formation and displacement of the vortex ring, caused by blade pitch, may be seen very distinctly.

Translated by Harry H. Heyson,
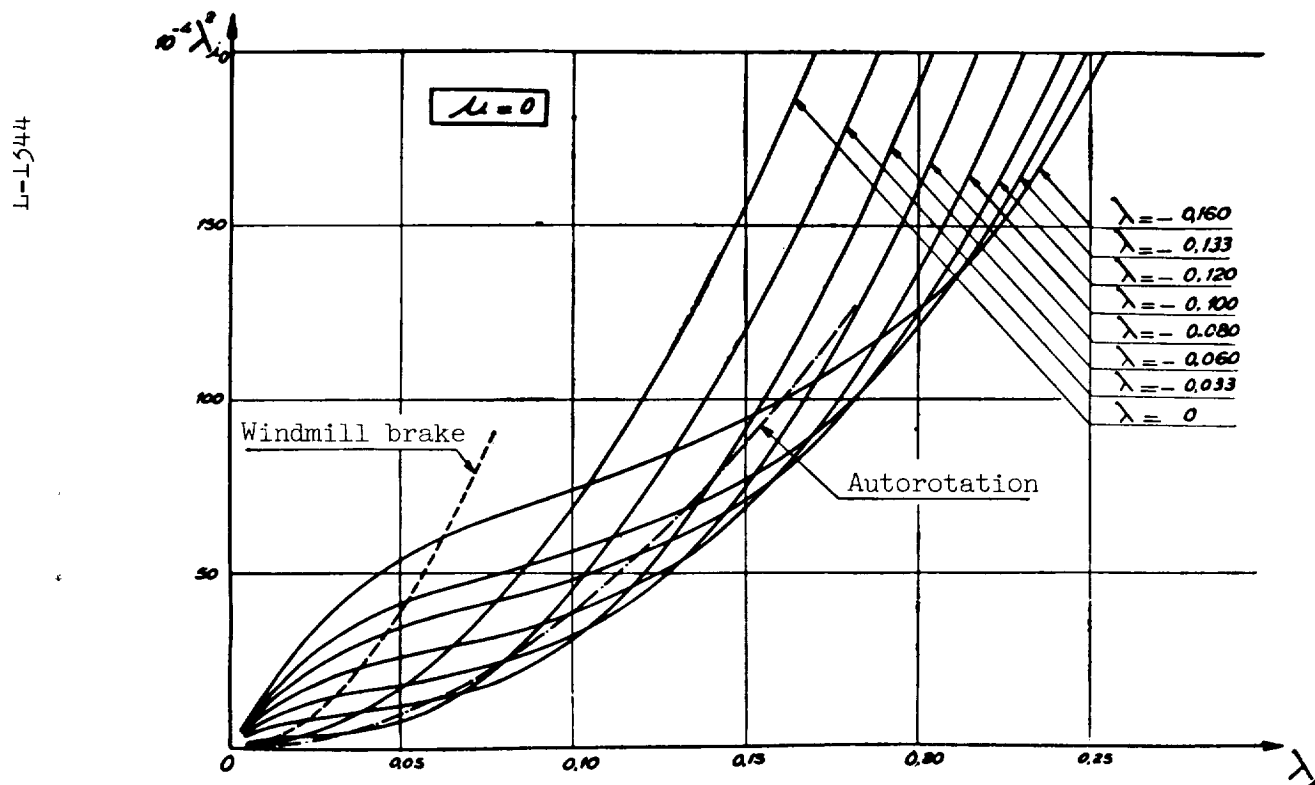National Aeronautics and Space Administration,
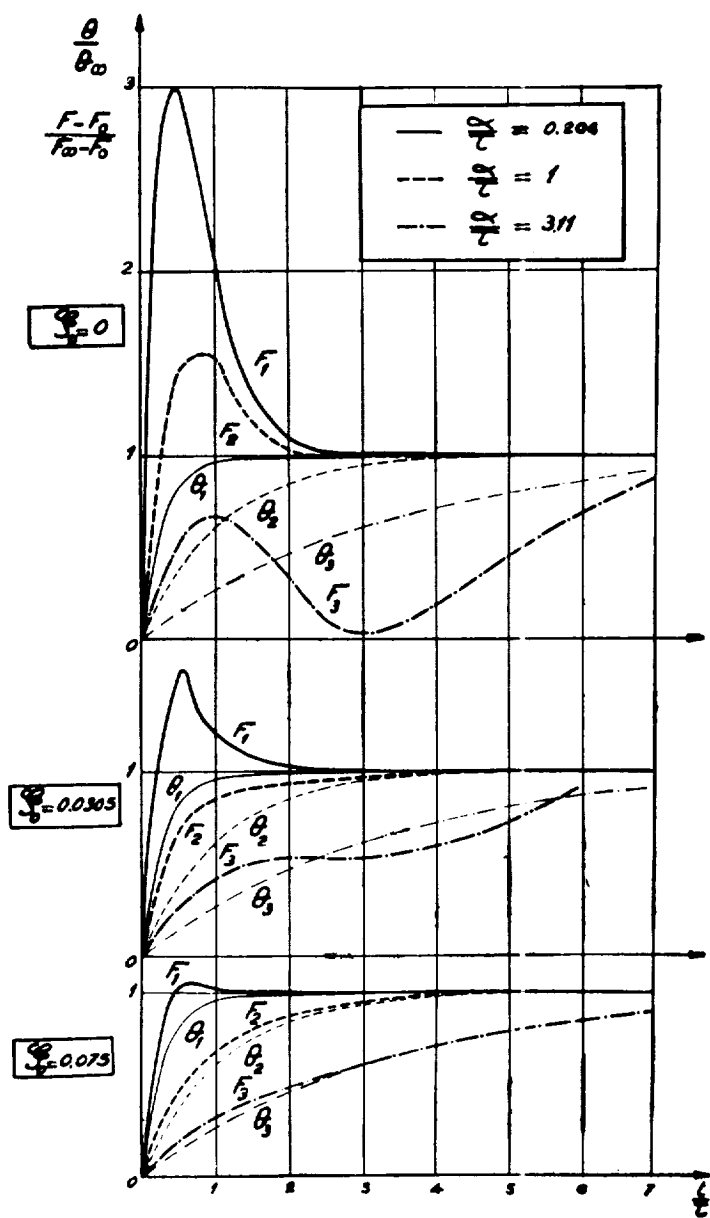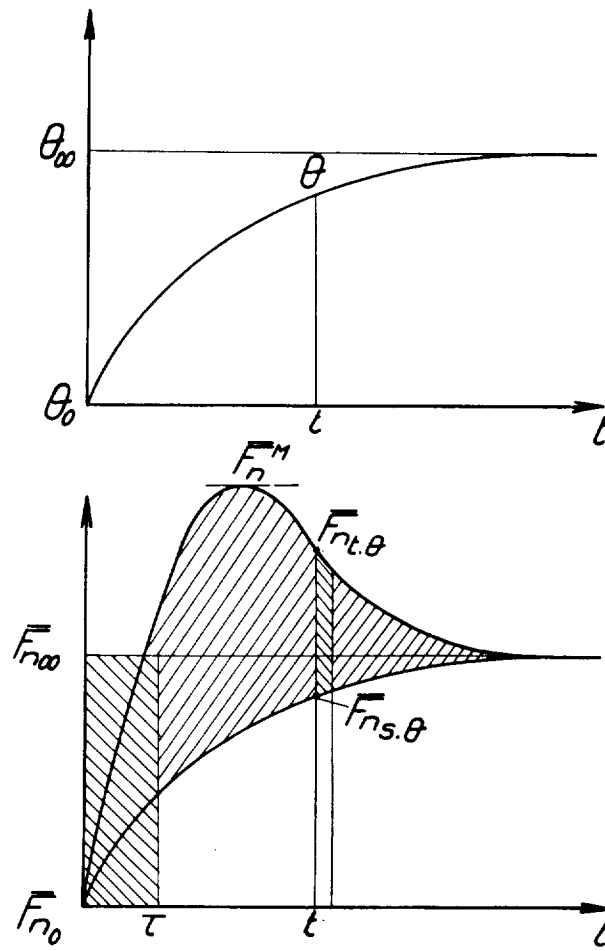Langley Field, Virginia.
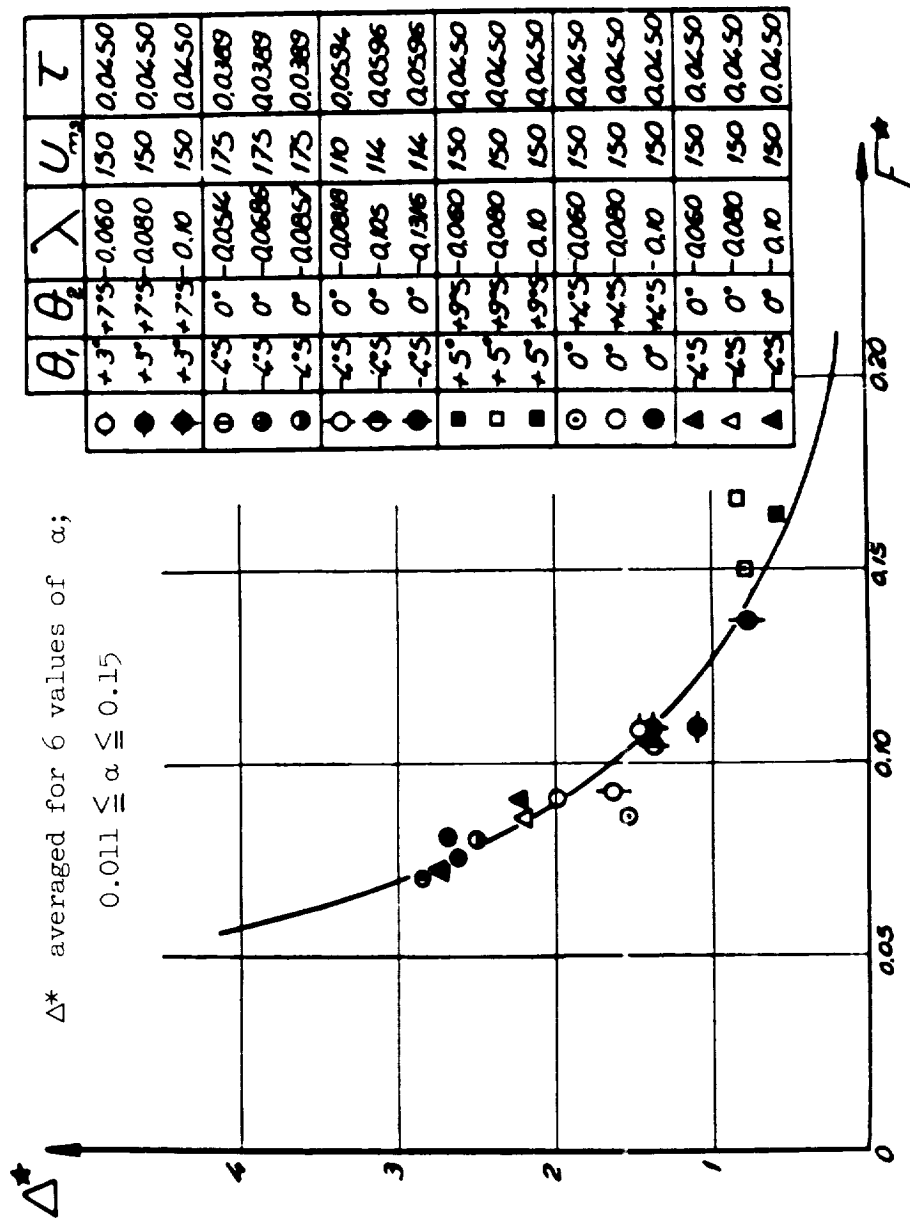
Figure 1.

Figure 2.

Figure 3.

16

Δ* averaged for 6 values of α;

0.011 ≤ α ≤ 0.15

	θ_1	θ_2	λ	U_{m_3}	T
○	+3°	+1°75	-0.060	150	0.0450
●	+3°	+1°75	-0.080	150	0.0450
◆	+3°	+1°75	-0.10	150	0.0450
◐	-1°5	0°	0.054	175	0.0369
●	-1°5	0°	-0.0688	175	0.0369
◑	-1°5	0°	-0.085	175	0.0369
○	-1°5	0°	0.0848	110	0.0594
◇	-1°5	0°	0.05	114	0.0596
◆	-1°5	0°	0.0945	114	0.0596
■	+5°	+1°75	-0.080	150	0.0450
□	+5°	+1°75	-0.080	150	0.0450
■	+5°	+1°75	-0.10	150	0.0450
⊙	0°	+1°5	-0.060	150	0.0450
○	0°	+1°5	-0.080	150	0.0450
●	0°	+1°5	-0.10	150	0.0450
▲	-1°5	0°	-0.060	150	0.0450
△	-1°5	0°	-0.080	150	0.0450
▲	-1°5	0°	-0.10	150	0.0450

Δ^*

F^*

Figure 4.

П-СТ-44

L-1544

$$\frac{F^N - F_0}{F_\infty - F_0}$$

$\frac{\tau}{\alpha} = 3$ $\frac{\tau}{\alpha} = 4.09$

$\frac{\tau}{\alpha} = 1.80$

$\frac{\tau}{\alpha} = 0.75$

$\frac{\tau}{\alpha} = 0.459$

$\frac{\tau}{\alpha} = 0.30$

o	$\frac{\tau}{\alpha}$	$= 0.30$
+	$\frac{\tau}{\alpha}$	$= 0.459$
●	$\frac{\tau}{\alpha}$	$= 0.750$
□	$\frac{\tau}{\alpha}$	$= 1.80$
◉	$\frac{\tau}{\alpha}$	$= 3$
▲	$\frac{\tau}{\alpha}$	$= 4.09$

3

2

1

0   0,05   0,10   0,15   0,20   0,25 F^*

Figure 5.

Figure 6.- Arrangement of setup.

Figure 7.- Rotor head with provisions for measuring the flapping
motions of the blades.
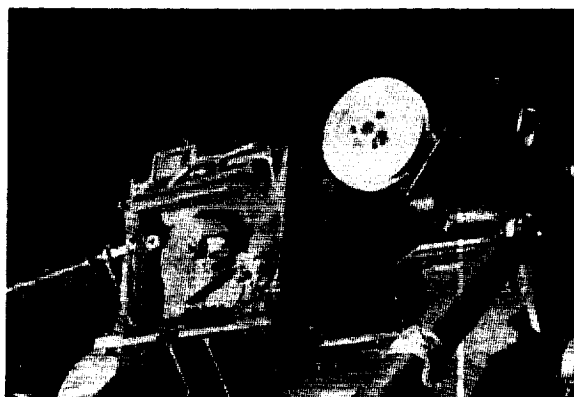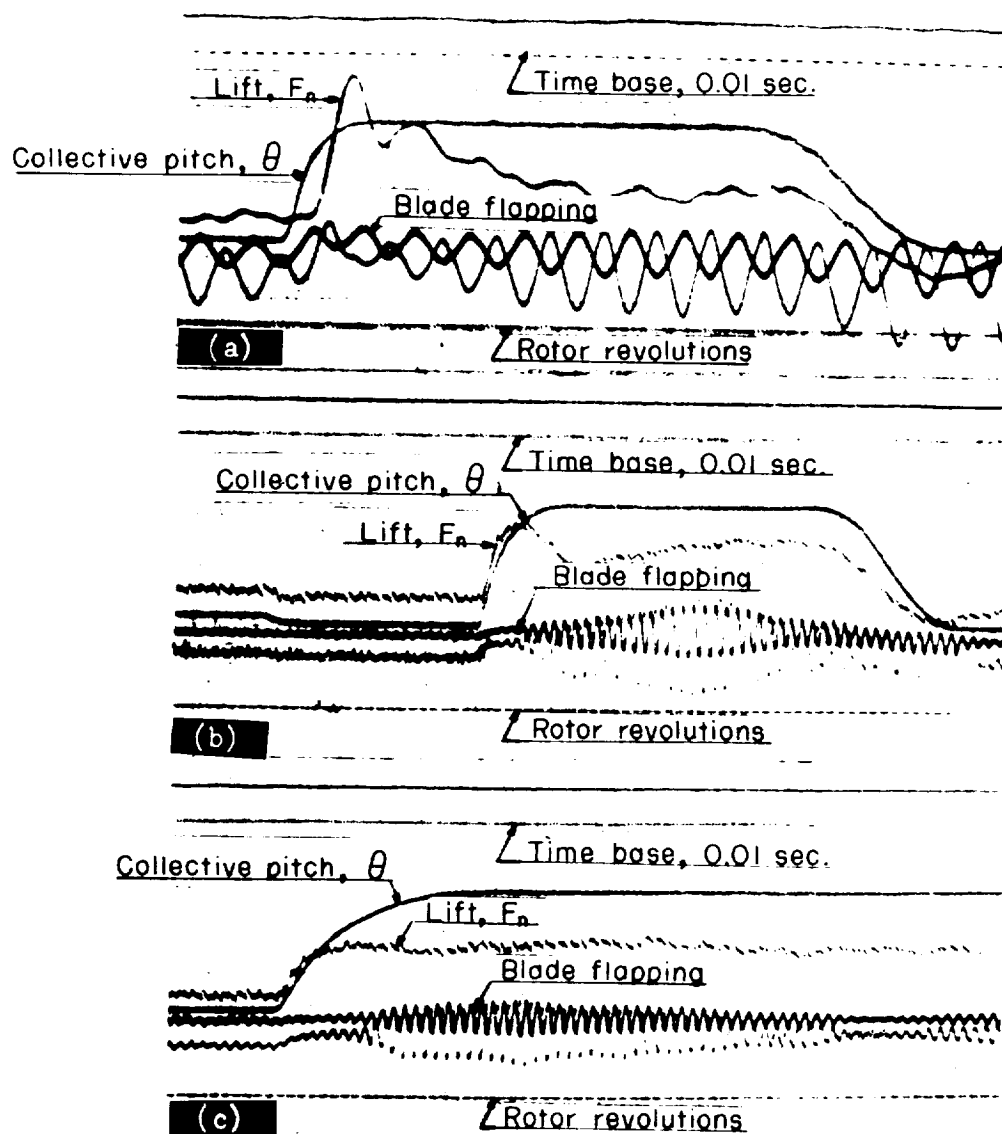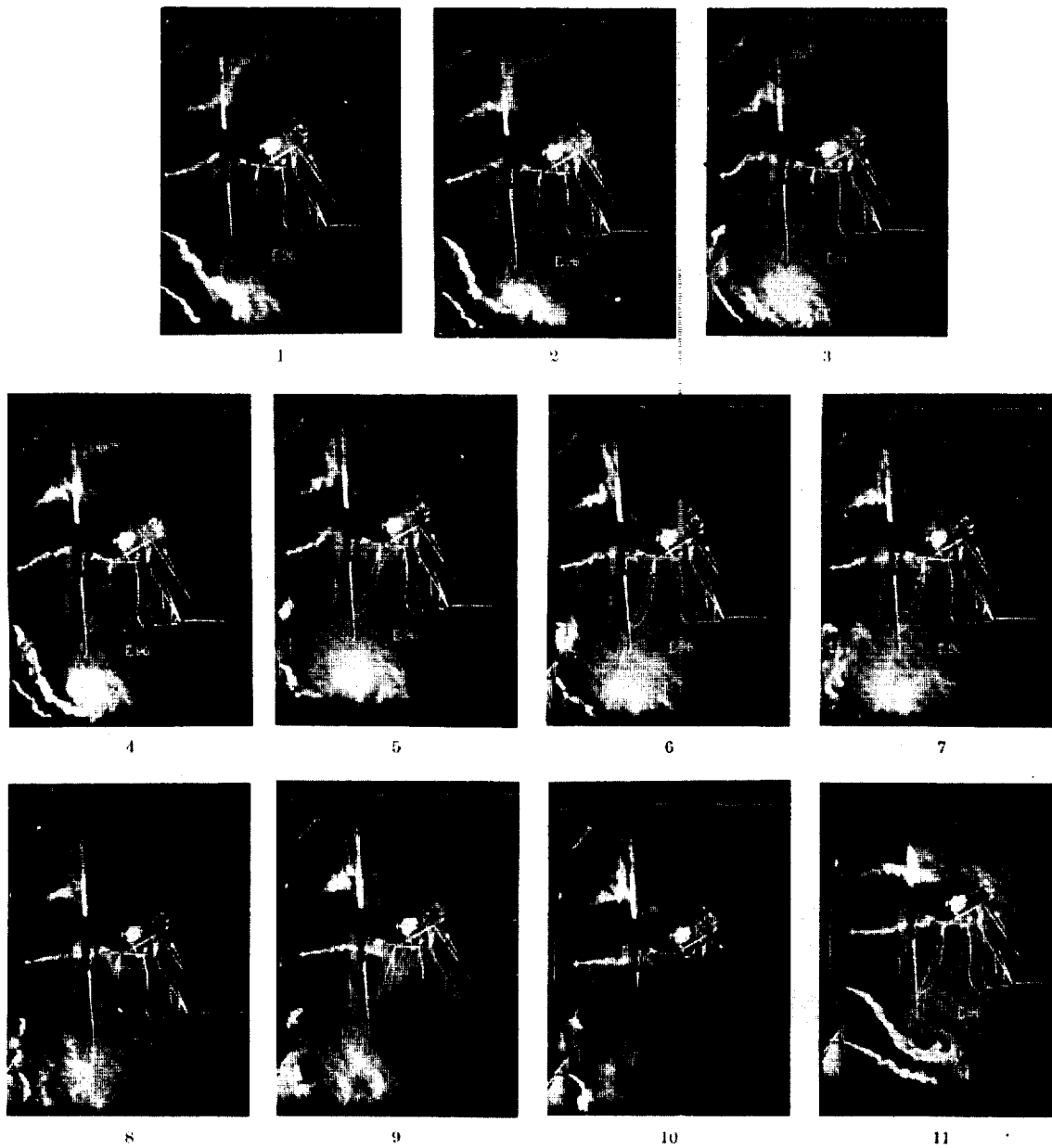

Figure 8.- Provisions for pitch change.

Figure 9.

Figure 10.- V = 150 ms, μ = 0, and λ = -0.06. Initial pitch θ_1 = 0°, final pitch θ_2 = $4^o5'$, and time for pitch change α_4 = 0.025 sec.